Proceedings of ASME Turbo Expo 2003
Power for Land, Sea and Air
June 16-19, Atlanta, Georgia, USA

GT2003-38303

UNSTEADY SURFACE PRESSURES DUE TO WAKE INDUCED TRANSITION IN A LAMINAR SEPARATION BUBBLE ON A LP TURBINE CASCADE

Rory Stieger[†]
Whittle Laboratory
Cambridge University
Cambridge, U.K.

David Hollis
Department of Aeronautical and Automotive Engineering
Loughborough University
Loughborough, U.K.

Howard Hodson
Whittle Laboratory
Cambridge University
Cambridge, U.K.

ABSTRACT

This paper presents unsteady surface pressures measured on the suction surface of a LP turbine cascade that was subject to wake passing from a moving bar wake generator. The surface pressures measured under the laminar boundary layer upstream of the steady flow separation point were found to respond to the wake passing as expected from the kinematics of wake convection. In the region where a separation bubble formed in steady flow, the arrival of the convecting wake produced high frequency, short wavelength, fluctuations in the ensemble averaged blade surface pressure. The peak-to-peak magnitude was 30% of the exit dynamic head.

The existence of fluctuations in the ensemble averaged pressure traces indicates that they are deterministic and that they are produced by coherent structures. The onset of the pressure fluctuations was found to lie beneath the convecting wake and the fluctuations were found to convect along the blade surface at half of the local freestream velocity. Measurements performed with the boundary layer tripped ahead of the separation point showed no oscillations in the ensemble average pressure traces indicating that a separating boundary layer is necessary for the generation of the pressure fluctuations.

The coherent structures responsible for the large amplitude pressure fluctuations were identified using PIV to be vortices embedded in the boundary layer. It is proposed that these vortices form in the boundary layer as the wake passes over the inflexional velocity profiles of the separating boundary layer and that the rollup of the separated shear layer occurs by an inviscid Kelvin-Helmholtz mechanism.

INTRODUCTION

The boundary layers of low-pressure (LP) turbine blades have received a great deal of attention due to the advent of high lift and ultra high lift LP turbines. The design of these turbines exploits unsteady transition phenomena, as described by Halstead et al [1]-[4], to reduce component counts at little or no efficiency penalty. Much of the understanding of unsteady transition is based on attached flow bypass transition and excellent reviews by Mayle [5] and Walker [6] provide extensive correlations built to predict transition in attached boundary layers. However, LP turbines operate at low Reynolds numbers, typically in the range 0.9 - 2×10^5, this coupled with high levels of boundary layer diffusion lead to the formation of a separation bubble under steady flow. The effect of wake passing has been shown by Schulte and Hodson [7] to periodically suppress the separation bubble. However the details of the unsteady transition mechanism in strong adverse pressure gradients and separating boundary layers remains poorly understood. The work of D'Ovidio et al [8] - [9] has extended the useful range of transition correlations but has not provided fundamental insight into the transition mechanism resulting from the interaction of a wake and laminar separation.

A detailed investigation into the unsteady boundary layer development has been conducted on the T106 LP turbine cascade in a bar passing rig to simulate the unsteady LP turbine environment at low speed. In particular the unsteady suction surface pressure distribution has been measured together with hot wire boundary layer traverses and PIV. Large amplitude pressure fluctuations were measured and were identified as being associated with rollup vortices formed by the wake passing over the inflexional boundary layer.

[†] Current address: Rolls-Royce plc, Derby, UK

NOMENCLATURE

C	chord
Cp	pressure coefficient $Cp=(P_0-P)/(P_0-P_{2is})$
f	bar passing frequency
f_r	reduced frequency $f_r=fC/V_{2is}$
P	local surface pressure
P_0	total pressure
P_{2is}	isentropic exit pressure
Re	Reynolds number $Re=V_{2is}C/\nu$
$Re_{\delta*}$	displacement thickness Reynolds number
s	distance along blade surface
s_0	suction surface length
s_b	bar pitch
s_c	cascade pitch
t	time
τ_0	bar passing period
U_b	bar speed
V_{2is}	isentropic exit velocity
V_{x1}	inlet axial velocity
$\delta*$	displacement thickness
f	flow coefficient $\phi=V_{x1}/U_b$
ν	kinematic viscosity

EXPERIMENTAL FACILITY AND TECHNIQUES

The measurements reported in this paper were made on the T106 LP turbine profile in a bar passing cascade at the Whittle Laboratory. The rig, shown in Figure 1, simulates the unsteady wake-passing environment of a LP turbine by traversing bars across the inlet flow. The wakes shed from these bars simulate the wakes of an upstream blade row in a multistage turbine. Details of the cascade are presented in Table 1 and further details of the bar passing cascade facility can be found in Stieger [10]. Also shown in Figure 1 is the light sheet location used for PIV measurements.

Chord	[mm]	198
Blade stagger	[°]	59.3
Pitch	[mm]	158
Span	[mm]	375
Inlet flow angle	[°]	37.7
Design exit flow angle	[°]	63.2
Bar diameter	[mm]	2.05
Axial distance: bars to LE	[mm]	70
Flow Coefficient (ϕ)		0.83

Table 1: T106 bar passing cascade details.

In this study the unsteady blade surface pressures were measured at mid span of the T106 cascade using four Kulite XCS-062 pressure transducers fitted with B screens and yielding a maximum frequency response of approximately 20kHz. The diameter of the Kulite is 1.6 mm, which corresponds to 0.6% of the suction surface length. The transducer was mounted in a brass sheath, which was screwed into the holes in the blade so that the transducer was flush with the surface as shown in Figure 2. The suction surface of the central blade of the T106 cascade was instrumented at 21 streamwise locations along the suction surface at mid span. Brass plugs were made for each of the vacant transducer locations. These plugs were polished flush with the surface of the blade.

Fylde 492BBS bridges were used to power the Kulite transducers and the bridge outputs were fed into Fylde 254GA amplifiers with a gain of 1000. A National Instruments PCI-MIO-16E-1 A/D card was used to measure the amplifier outputs. Only the fluctuating pressure was measured by the Kulites. On-line calibration of the transducers, bridges and amplifiers was performed simultaneously using a Druck DPI520 as a pressure source. The system described above resulted in a sensitivity of approximately 500Pa/V, with a discretisation error of 0.05Pa. Each measurement of the fluctuating pressure consisted of 256 ensembles of 4096 points logged at 10KHz.

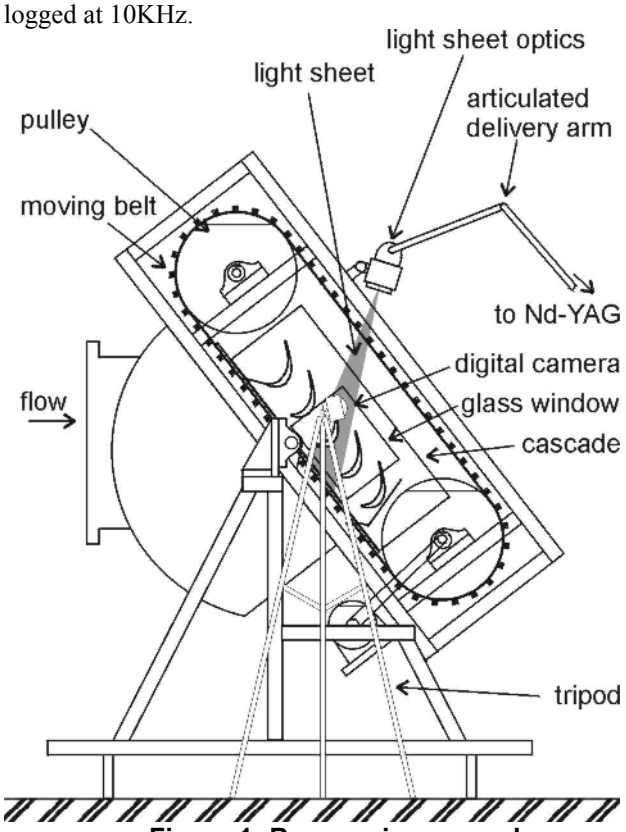

Figure 1: Bar passing cascade.

Pneumatic static pressure tapings, located at 25% span, were used to determine the mean pressure level at each of the Kulite locations. Oil and dye flow visualization showed that the static pressure tappings were within the 2D flow region on the cascade.

The mean pressure level was measured using a Scanivalve DSA 3017 array with a ±10 in H_2O range and 16-bit A/D. The discretisation error on this measurement is thus 1.0 Pa which corresponds to 1.0% exit dynamic head at the nominal flow condition of $Re=1.6\times10^5$. The voltage outputs of the Kulites were converted to pressure by a linear calibration, before

ensemble averaging and adding the mean pressure measured by the DSA. The results were non-dimensionalised by isentropic exit dynamic head to give the ensemble averaged pressure coefficient.

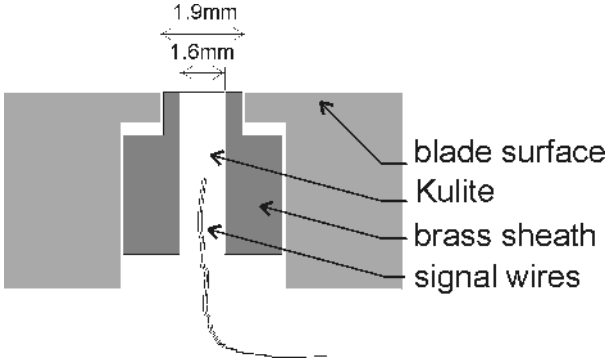

Figure 2: Mounting of pressure transducers to measure unsteady blade surface pressure.

PIV measurements were made using a commercial TSI PIV system. A pair of 50mJ New Wave Nd-YAG lasers delivered light to the terminal optics via an articulated delivery arm. A 25.4mm focal length negative cylindrical lens and a 500mm focal length spherical lens were used to generate the light sheet that was between 0.5mm and 1.5mm thick on the blade surface.

A Kodak digital camera with 1024×1024 CCD array was used to acquire the images through a 105mm Nikon lens providing a 19.0mm square field of view. The inter frame delay was set to Δt=3ms, which gave particle displacements in the range 3 to 6 pixels. The maximum data rate of the PIV system was 15Hz so it was not possible to capture a sequence of images within one bar passing cycle. A trigger signal generated by the bar passing was passed through a delay generator thereby allowing the PIV images to be acquired at selected phases relative to the bar passing trigger.

The flow was seeded with a mist of groundnut oil generated by a pair of TSI Six-Jet Atomisers. The seeding was introduced into plenum chamber of the wind tunnel approximately 3m upstream of the bar passing cascade.

The acquired image pairs were processed using LaVision's DaVis V.6.03 software (LaVision, [11]). An adaptive multi-pass technique was used with the initial cell size of 64×64 pixels decreasing to a final cell size of 16×16 pixels with a spatial resolution of 304μm×304μm. The final cells were overlapped by 50% effectively increasing the data yield and giving a vector grid spacing of 152μm.

The arrangement of the light sheet and the camera is shown in Figure 1. The position of the light sheet optic was chosen so that shadows from the returning bars of the wake generator were not present at the phases of interest. The light sheet optic was also positioned out of the main exit flow to minimise blockage. The camera was positioned to look parallel to the blade surface through the glass sidewall to minimise flare.

TIME MEAN SURFACE PRESSURE DISTRIBUTION

The surface distribution of static pressure coefficient, C_p, is shown in Figure 3 for four different configurations together with the envelope of unsteady pressures measured for the case s_b/s_c=1. For steady inflow, the pressure distribution is shown for both the suction and pressure surfaces. Peak suction is located at s/s_0=0.45. A laminar separation bubble is evident over the rear portion of the suction surface with separation at s/s_0=0.60. The pressure plateau, typically associated with the laminar shear layer of a steady separation bubble, extends to s/s_0≈0.82. At this location the pressure begins to recover as the separated shear layer undergoes transition and reattaches by s/s_0=0.88.

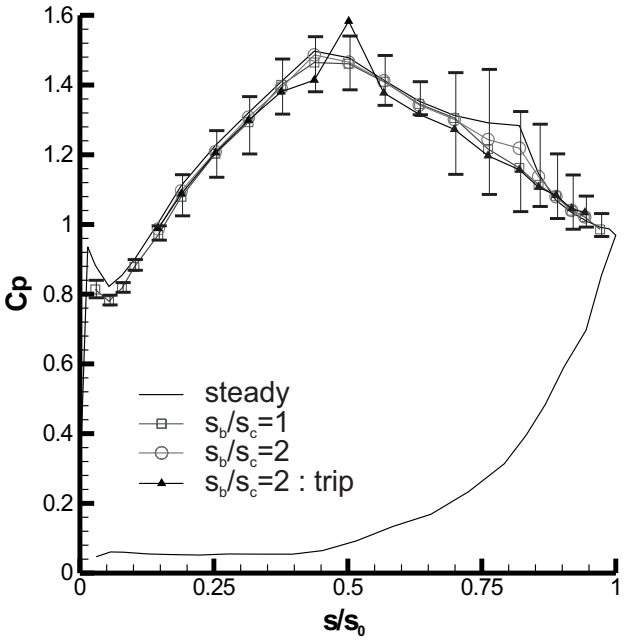

Figure 3: Pressure distribution measured on the T106 cascade at Re=1.6×10^5.

For both cases with incoming wakes, only the suction surface C_p distribution is shown. For the case of s_b/s_c=1 (f_r=0.68) the time-mean surface pressure distribution shows no sign of the separation bubble. In the time-mean, the separation bubble has been suppressed by the wakes. For the case of s_b/s_c=2 (f_r=0.34), where the steady state boundary layer has more opportunity to re-establish between wake passing events, the time average surface pressure distribution indicates the presence of a separation bubble. The separation and reattachment point for this case are indistinguishable from the case for steady inflow; however, the pressure plateau is not as prevalent as in the steady flow case. This is due to the pneumatic averaging of the measurement system. The flow is periodically attached by the presence of the passing wake. The final surface pressure distribution on Figure 3 is for the case of s_b/s_c=2 with the boundary layer tripped by a 0.056 mm diameter wire attached to the blade surface at s/s_0≈0.44. The resulting turbulent boundary layer shows no signs of separation. The C_p

distribution is altered by the presence of the trip wire, with local deceleration and acceleration before and after the trip-wire.

Near the leading edge of the suction surface, the C_p distributions differ for the steady inflow case and the cases with bar passing. The differences are due to an effective change in incidence of the incoming flow due to the bars of the wake generator turning the inlet flow. This alteration of the incidence is small and does not significantly alter the pressure distribution downstream of peak suction, which is the region of primary interest. Nor, as the later results will show, does it affect the boundary layer that enters this region.

ENSEMBLE-AVERAGE SUCTION SURFACE PRESSURES

The ensemble averaged unsteady surface pressures measured on the suction surface for the case of $s_b/s_c=1$ are presented as contours of C_p on an ST diagram in Figure 4. The convection of the wake is evident and, upstream of the separation point, is explained in terms of the negative jet model of Meyer [12]. The negative jet, incident on the suction surface, causes the surface pressure to increase locally as the wake convects over the suction surface. The increase in surface pressure corresponds to the reduction in C_p observed in Figure 4.

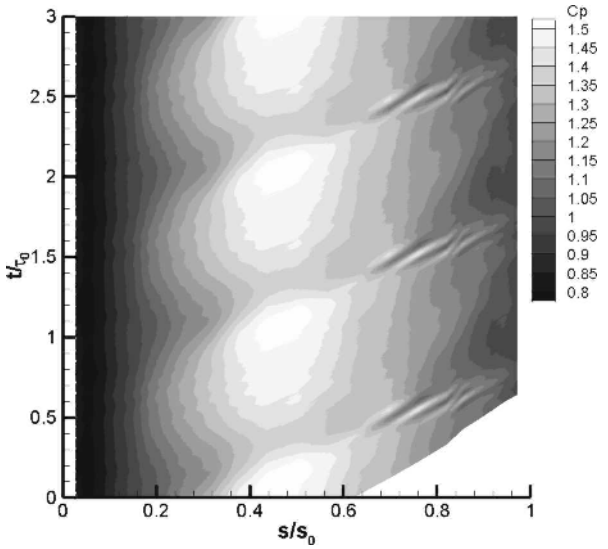

Figure 4: ST diagram of ensemble average C_p. Re=1.6×10^5, s_b/s_c=1

The nature of the pressure traces in the region where the wake passes the steady flow separation bubble is markedly different from upstream where the boundary layer is laminar and attached. The fact that these pressure fluctuations are evident in the ensemble-averaged pressure traces indicates that they are formed by deterministic coherent flow structures. As the wake arrives at the steady flow separation location, a series of large amplitude pressure oscillations arise. At s/s_0=0.76 the peak-to-peak amplitude of these pressure fluctuations is ΔC_p=0.3. It should be noted that the contours of Figure 4 are drawn with the mesh aligned at half the mean flow velocity. This reduces the aliasing due to the contour algorithm that results from the temporal resolution being much finer than spatial resolution.

Ensemble averaged pressure traces measured over the rear half of the suction surface, are shown in Figure 5. This is a portion of the data shown in Figure 4. Here, the dash-dot lines indicate the surface location of each Kulite while the solid lines are the ensemble-averaged traces of the measured surface pressure fluctuation. The vertical scale of the pressure traces is arbitrary but the same for all of the traces.

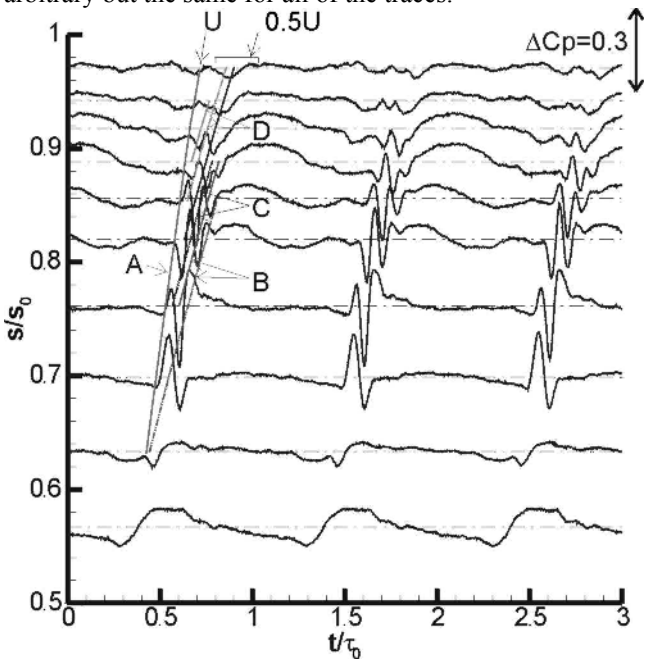

Figure 5: Ensemble average pressure traces measured over the rear of the suction surface. Re=1.6×10^5, s_b/s_c=1

The line, labelled A, in Figure 5 is a trajectory line drawn at the freestream velocity. The onset of the large amplitude pressure oscillations in Figure 5, fall along line A showing that the onset of the pressure oscillations is dictated by the wake convecting with the freestream. The onset of the pressure oscillations is thus not controlled by the convection of turbulent spots nor instability waves within the boundary layer as these phenomena convect slower than the freestream. It can also be deduced that the onset is not controlled by an acoustic mechanism as for a low Mach number flow these would travel ahead of the convecting wake.

The pressure fluctuations are observed to originate between the transducers located at s/s_0=0.57 and s/s_0=0.63. The amplitude of the fluctuations increases up to s/s_0=0.70 and thereafter remains approximately constant. The period of the oscillations is also constant downstream of s/s_0=0.70. The amplitude of the fluctuations reduces slightly downstream of s/s_0=0.82. This region corresponds to the pressure recovery region of the steady separation bubble and is typically associated with transition in a separation bubble. With increased levels of turbulence and turbulent mixing that results

from transition, the ensemble-average pressure fluctuations decrease in amplitude.

The trajectory lines labelled B and C are drawn at half the local freestream velocity. These lines are positioned to trace the convection of the maxima and minima of the pressure fluctuations and show that the coherent structures responsible for the pressure fluctuations travel at half the freestream velocity.

The number of maxima and minima in the ensemble averaged pressure traces is not the same at every sensor location in Figure 5. At s/s_0=0.70 there is only one maxima and one minima observed, however, at s/s_0=0.82 there are three sets of maxima and minima. The appearance of more than one coherent structure is due to the different trajectories of the onset and convection of the structures. Once formed the structures convect slower than the wake thus allowing the wake to generate new structures at points further downstream as it passes over the undisturbed inflexional profiles of the separating boundary layer.

By extending the trajectory lines C to intersect line A, the origin of line C is seen to be at $s/s_0 \approx 0.60$. However, by $s/s_0 \approx 0.86$ the feature occurring along line C disappears. The convection speed of C is lower than the convection speed of the leading edge of a turbulent spot. The disappearance of C is attributed to turbulent spots formed at an upstream location in the boundary layer overtaking the coherent structure. This turbulence destroys the coherence of structure C.

The effect of bar passing frequency

Figure 6 shows the ensemble averaged unsteady surface pressures for the identical flow condition in Figure 5, but with double the bar spacing so that s_b/s_c=2 (f_r=0.34). Both the time axis and the scale of the pressure traces are identical to that of Figure 5.

The pressure fluctuations are again observed as the wake passes over the region of the steady flow separation bubble. No change in the onset location is evident and the period of oscillation is the same as before. The period of the pressure fluctuations are thus independent of the wake passing frequency in the range relevant for LP turbines. The pattern of the pressure oscillations is also the same as for the higher bar passing frequency up to s/s_0=0.86 but their magnitude is larger for the lower bar passing frequency.

The lower bar passing frequency gives the boundary layer more time to re-establish steady state conditions between the wake passing events. In this time a series of pressure oscillations, smaller in magnitude and of lower frequency arise downstream of s/s_0=0.88. The pattern of these pressure traces is different to those resulting from the wake-separation bubble interaction and are more nearly sinusoidal. The fact that these oscillations may be ensemble averaged is remarkable and indicates that they too are deterministic and caused by coherent structures in the re-establishing boundary layer. Based on Stieger and Hodson's [13] observations of Tollmien-Schlichting waves on a flat plate with identical pressure distribution, it is proposed that these oscillations in surface pressure are due to natural transition phenomena.

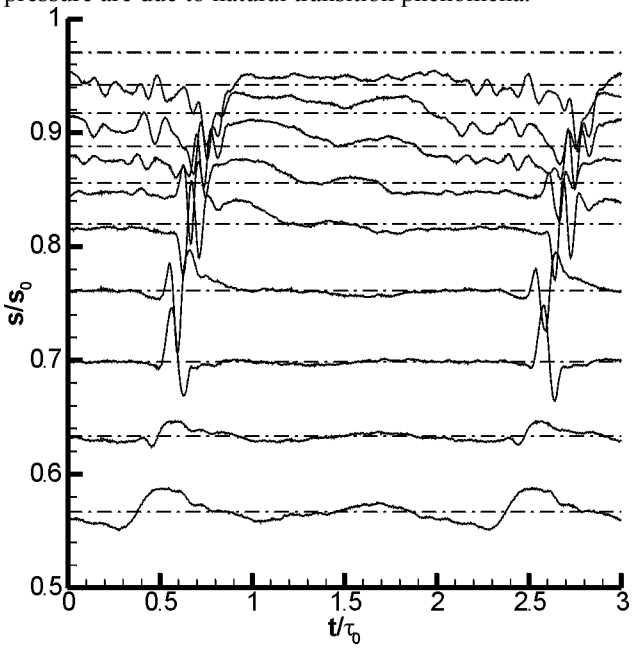

Figure 6: Ensemble average pressure traces for $Re=1.6\times10^5$, s_b/s_c=2.

The effect of a boundary layer trip

A trip wire was fixed to the surface of the blade to cause transition of the boundary layer so that downstream of the trip wire, the boundary layer is turbulent throughout the wake passing cycle suppressing the formation of a separation bubble. Figure 7 shows ensemble averaged pressure traces for identical flow conditions to those presented in Figure 6, but with a trip wire at s/s_0=0.44. Immediately obvious is the absence of the pressure fluctuations. The coherent structures responsible for the pressure fluctuations are thus only formed when the wake interacts with the separating boundary layer.

The effect of Reynolds number

It was established above that the period of the large amplitude pressure fluctuations is independent of the bar passing frequency. However, the period of the pressure fluctuations is dependent on Reynolds number. The pressure traces at a Reynolds number of $Re=1.6\times10^5$ and at a Reynolds number $Re=2.0\times10^5$, are compared at s/s_0=0.70 in Figure 8 where the period of interest is shown on a dimensional time axis. It is apparent that the period of the pressure oscillations is not the same at the different Reynolds numbers. The time offset between the two sets of pressure traces is due to difference in the absolute time of the trigger used for the ensemble averaging of the different Reynolds number flow conditions. The period of oscillations at s/s_0=0.70 are approximately inversely proportional to the Reynolds number.

The convective time scale,

$$\tau_{conv} \propto \frac{C}{U} \quad (1)$$

and viscous diffusion time scale,

$$\tau_{visc} \propto \frac{\delta^{*2}}{\nu} \propto \frac{\left(\frac{x}{\sqrt{\mathrm{Re}_x}}\right)^2}{\nu} \propto \frac{x}{U} \quad (2)$$

are indistinguishable for a given velocity distribution as the ratio of local surface position to chord is constant. It is thus not possible to determine if the large pressure fluctuations are related to viscous or convective phenomena.

A correlation for the period of the disturbance with the maximum amplification rate in the Falkner-Skan velocity profiles over the whole range of pressure gradient parameter is given by Walker [14] as

$$\tau_{crit} \propto \frac{1}{f_{crit}} = \frac{\nu}{3.2\,\mathrm{Re}_{\delta^*}^{-3/2} U^2} \quad (3)$$

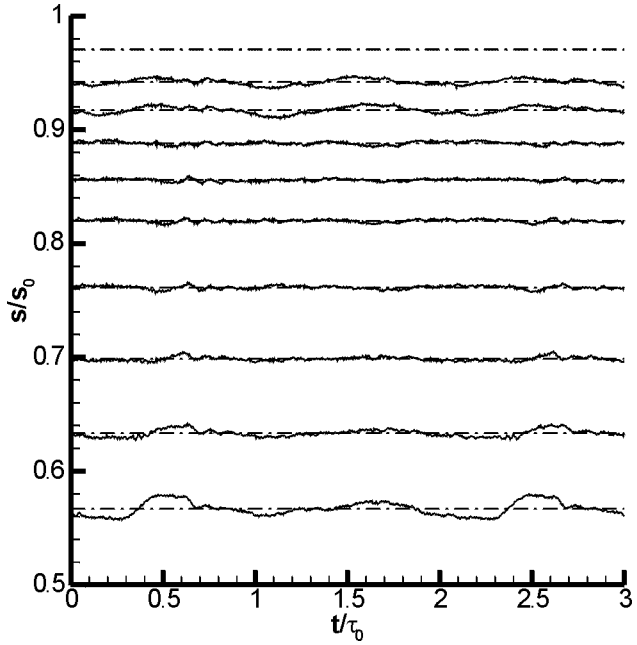

Figure 7: Ensemble average traces - tripped boundary layer, Re=1.6×10^5, s_b/s_c=2.

This correlation was shown by Stieger and Hodson [13] to reasonably predict the frequency of Tollmien-Schlichting waves in similar unsteady flow conditions. The period of a viscous instability in a highly decelerated boundary layer is thus expected to vary non-linearly with Reynolds number. The observed linear relationship between the period of the pressure fluctuations and Reynolds number demonstrates that a viscous stability mechanism is not responsible for the large amplitude pressure fluctuation. Villermaux [15] showed that inviscid instability processes have a negligible Reynolds number dependence and so a pure inviscid instability mechanism is excluded.

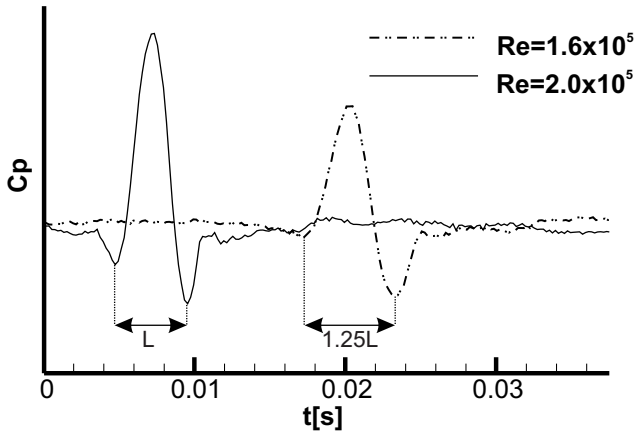

Figure 8: Effect of Reynolds number on the period of pressure oscillations at s/s_0=0.70.

VISUALISATION OF THE INSTANTANEOUS FLOW FIELD USING PIV

PIV is essentially a quantitative flow visualisation technique whereby the correlation of two images of a seeded flow is used to determine the fluid velocity. In order to identify the structures responsible for the pressure fluctuations presented above PIV measurements were made over a small portion of the rear suction surface of the T106 cascade as shown in Figure 9.

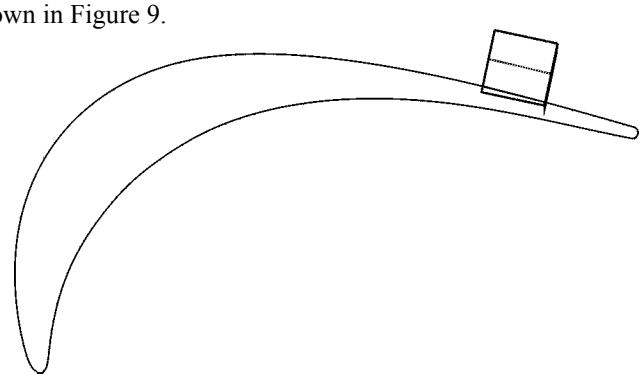

Figure 9: Location of PIV measurement on the T106 blade. The line dividing the field of view indicates the portion of the measurement shown below.

The results of a PIV measurement in the region between s/s_0=0.8 and s/s_0=0.9 at the phase t/τ_0=0.85 are shown in Figure 10. The instantaneous vector map is shown in the upper plot of Figure 10. Two vortices are visible in the boundary layer. Instantaneous streamlines calculated from the vector map are shown in the lower plot of Figure 10 and confirm that the structures are vortices embedded in the boundary layer. A number of PIV measurements were made and not all showed identical features to the results of Figure 10. The vortices were not always evident and their size and position varied.

The vorticity of the vortices is of the same sense as the boundary layer vorticity. The vortex centres are separated by approximately 5% of the suction surface length with their centres at approximately a third of the local time average

boundary layer thickness. It is argued below that these vortices are responsible for the measured pressure fluctuations.

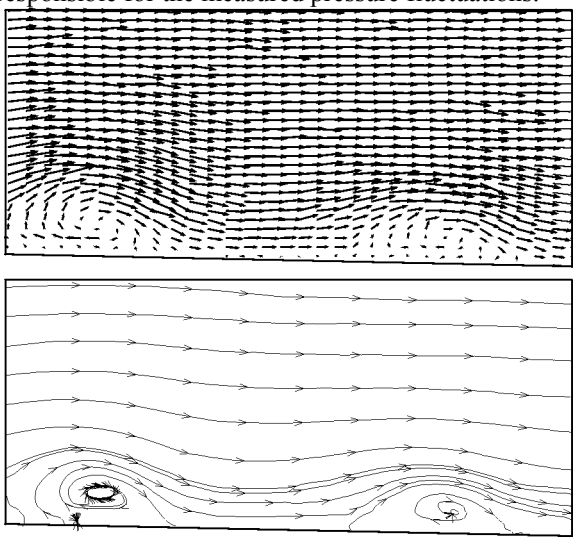

Figure 10: Instantaneous vector map and computed streamlines from PIV measurement over the rear suction surface at t/τ_0=0.85. Re=1.6×10^5, s_b/s_c=1.

THE SOURCE OF PRESSURE FLUCTUATIONS

Saathoff and Melbourne [16] conducted an investigation into the cause of large pressure fluctuations occurring near the leading edges of sharp-edged bluff bodies. A long two-dimensional rectangular prism was mounted in a wind tunnel and the surface pressure was measured under the separation bubble that formed at the leading edge. Flow visualisation was performed with a laser light sheet and high-speed cine camera. The cine camera was used to simultaneously capture flow visualisation pictures and an oscilloscope output from the pressure transducers. The results showed that large surface pressure fluctuations were caused by vortices in close proximity to the surface of the model. The rollup of the separated shear layer, initiated by perturbations in the approaching flow, was identified as the source of these vortices.

Luton et al [17] conducted a numerical investigation of the interaction of a convected spanwise vortex and a Blasius boundary layer. By solving the full Navier-Stokes equations, they showed a minimum in surface pressure to coincide with the location of the vortex centre. The magnitude of the pressure fluctuations associated with the vortex was shown to depend on the distance of the vortex from the wall as well as the strength of vortex. They reported fluctuations as high as 55% of the dynamic head for one of the cases calculated.

The measurements presented here are thus confirmed by the literature and the vortices identified by the PIV flow visualisation are responsible for the large amplitude pressure fluctuations measured on the surface of the T106 cascade.

THE FORMATION OF COHERENT STRUCTURES IN BOUNDARY LAYERS

The classical studies in boundary layer stability conducted by Schubauer and Skramstad [18] provided experimental evidence of coherent structures in boundary layers, in this case 2D Tollmien-Schlichting waves evolving from disturbance generated by a vibrating ribbon. The development of a small square wave disturbance in a Blasius boundary layer was investigated experimentally by Gaster [20] In this case, the disturbance was found to develop into a downstream propagating wave packet. Gaster found that the initial structure of the wave packet was well predicted by tracking the development of the amplified wave numbers using linear stability theory. The linear instability mechanism associated with the boundary layer lead to the amplification of particular frequencies. The exponential amplification rate associated with these frequencies lead to the dominance of the most amplified mode. Such a selective amplification process acts as a filter that leads to a single mode becoming dominant and this leads to the formation of a coherent structure being formed in the boundary layer, in this case a travelling wave packet.

Watmuff [19] conducted a detailed hot-wire and flying cross wire measurements of the evolution of a periodically applied point disturbance in a boundary layer with a laminar separation bubble. Despite an initial region of decay, the disturbance was found to amplify after the separation point before developing into a three-dimensional rollup vortex loop embedded in the boundary layer. Furthermore, the vortex structure was discernable up to 20 boundary layer thicknesses downstream of the time mean reattachment point. The maximum amplitude of the disturbance was observed to follow the trajectory of the inflexion points in the velocity profile and contours of the measured spanwise vorticity, along the centreline of the disturbance, revealed a cat's eye pattern, characteristic of a Kelvin-Helmholtz breakdown of the shear layer. This evidence allowed Watmuff to conclude that the instability mechanism governing the amplification of the wave packet in a separation bubble is predominantly inviscid.

The work of Gaster [20] and Watmuff [19] shows that the selective amplification associated with boundary layer stability, both viscid and inviscid, provides a mechanism able to select and amplify particular disturbance frequencies that subsequently form coherent structures in the boundary layer. It is proposed that the deterministic coherent structures responsible for the measured pressure fluctuations, namely the rollup vortices identified by the PIV measurements are formed by the selective amplification of such an instability mechanism. By contrast to the measurements of Watmuff [19], the wake is a uniform 2D disturbance and as a consequence it is expected that the rollup would initially be two dimensional and uniform across the span of the blade in the bar passing cascade.

THE MECHANISM OF SURFACE PRESSURE OSCILLATIONS

An overview of the mechanism whereby pressure fluctuations are formed is presented in Figure 11. The central plot shows the measured mean pressure distribution over the rear suction surface of the T106 LP turbine cascade for steady flow. Also shown is the hypothetical inviscid pressure distribution. Short portions of the ensemble averaged time traces of surface pressure are also shown for each measurement location. The lower plot shows a series of measured hot wire boundary layer profiles at different positions in the separation bubble corresponding to the boundary layer state just before the arrival of the wake. The dotted line, drawn by hand, passes approximately through the inflexion points of these boundary layer profiles. Just before the arrival of the wake, the laminar shear layer extends from the steady separation point to the end of the pressure plateau (from $s/s_0 \approx 0.60$ to $s/s_0 \approx 0.82$). The final set of profiles at $s/s_0=0.88$ does not have an inflexion point at any time during the wake passing cycle. This is representative of the reattached boundary layer after a separation bubble. This description of the profiles prior to the arrival of the wake agrees with what would be expected for a separation bubble within a steady flow and a free laminar shear layer exists before the arrival of the wake.

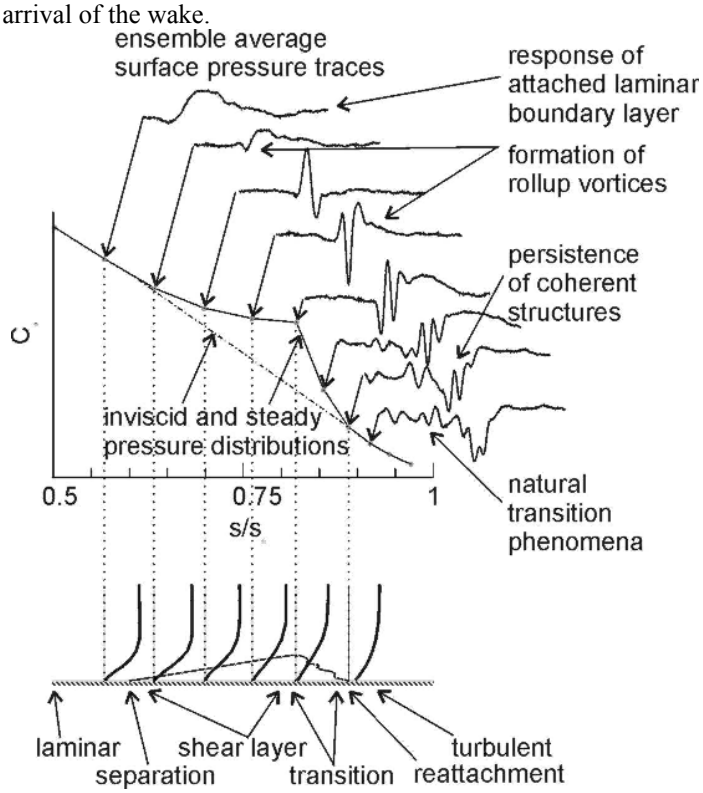

Figure 11: Schematic showing the evolution of pressure oscillations due to the interaction of the wake and separating boundary layer.

Between $s/s_0=0.63$ and $s/s_0=0.70$ the amplitude of the pressure fluctuations due to the wake passing rises significantly. Prior to the arrival of the wake, the boundary layer profiles are inflexional over this region of the blade surface. The intense amplification observed in this region is attributed to the instability mechanism resulting from the inflexional velocity profiles.

By $s/s_0=0.70$ the free shear layer has rolled up into a series of rollup vortices. The point disturbances in Watmuff's work were observed to grow laterally in the adverse pressure gradient and form vortex loops, however, for the case of wake passing, where the disturbance sources may be viewed as a two-dimensional strip of convecting wake fluid, the amplified disturbances would not break down into vortex loops, but rather a more two-dimensional spanwise rollup vortex. Rollup vortices formed in a shear layer convect at about the mean velocity of the shear layer, which would be approximately half the freestream velocity. The coherent structures responsible for the pressure fluctuations were previously identified to convect at half the freestream velocity. This further supports the argument that the coherent structures responsible for the large amplitude surface pressure fluctuations are rollup vortices formed in the separated shear layer associated with the inflexional boundary layer velocity profiles.

The pressure fluctuations labelled 'natural transition phenomena' in Figure 11 are believed to be caused by Tollmien-Schlichting type waves. As would be expected, the pressure traces observed in this region have a different character to those associated with the rollup vortices.

CONCLUSIONS

Measurements of the unsteady surface pressure on the T106 LP turbine cascade showed the laminar boundary layer upstream of the steady flow separation point to respond to the wake passing in an essentially inviscid manner. However, unexpected large amplitude fluctuations in surface pressure were measured as the wake convected over the region of the steady flow separation bubble. The pressure oscillations were suppressed when the boundary layer was tripped indicating that a separating laminar boundary layer was necessary for the development of the pressure oscillations. The pressure oscillations were found to be generated as the wake passed over the region covered by the separation bubble in the case of steady flow and to convect at half the local freestream velocity. The pressure oscillations were unaltered by a change in the bar passing frequency.

PIV measurements were used to identify vortices present in the boundary layer. It was confirmed by reference to literature that these vortices are responsible for the pressure oscillations.

In the ensemble-averaged measurements, the vortices appear as coherent and deterministic structures. Hot wire boundary layer traverses confirmed the existence of inflexional velocity profiles prior to the arrival of the wake. It is proposed that the instability mechanism associated with the inflexional velocity profiles amplifies perturbations to the laminar shear layer caused by the wake passing. This amplification leads to the formation of rollup vortices embedded in the boundary

layer and these rollup vortices are responsible for the large amplitude pressure fluctuations.

ACKNOWLEDGMENTS

The authors would like to thank John Black for providing access to the PIV equipment and for his help in setting up the PIV. The first author is also indebted to financial support provided by the ORS and the Peterhouse Research Studentship. The funding of EPSRC grant GR/L96660/01 is also gratefully acknowledged.

REFERENCES

[1] Halstead, D.E., Wisler, D.C., Okiishi, T.H., Walker, G.J., Hodson, H.P., Shin, H.-W., 1997 a, "Boundary layer development in axial compressors and turbines: Part 1 of 4 - Composite Picture," Journal of Turbomachinery, **119**, pp114-127, January

[2] Halstead, D.E., Wisler, D.C., Okiishi, T.H., Walker, G.J., Hodson, H.P., Shin, H.-W., 1997 b, "Boundary layer development in axial compressors and turbines: Part 2 of 4 – Compressors," Journal of Turbomachinery, **119**, pp114-127, January

[3] Halstead, D.E., Wisler, D.C., Okiishi, T.H., Walker, G.J., Hodson, H.P., Shin, H.-W., 1997 c, "Boundary layer development in axial compressors and turbines: Part 3 of 4 - LP Turbines," Journal of Turbomachinery, **119**, pp114-127, January

[4] Halstead, D.E., Wisler, D.C., Okiishi, T.H., Walker, G.J., Hodson, H.P., Shin, H.-W., 1997 d, "Boundary layer development in axial compressors and turbines: Part 4 of 4 - Computations and Analyses," Journal of Turbomachinery, **119**, pp114-127, January

[5] Mayle, R.E., 1991, "The role of laminar-turbulent transition in gas turbines engines," ASME Journal of turbomachinery, **113** October , 13/509.

[6] Walker, G.J., 1993, "The role of laminar turbulent transition in gas turbine engines: a discussion," ASME Jnl. Turbomachinery, **115**, pp 207-217, April

[7] Schulte, V. and Hodson, H.P., 1998, "Unsteady wake-induced boundary layer transition in high lift LP turbines," ASME Journal of Turbomachinery **120**, pp28-35. January

[8] D'Ovidio, A., Harkins, J. A., Gostelow, J. P., 2001 a, "Turbulent spots in strong adverse pressure gradients: Part 1 - Spot Behavior," Proceedings of ASME TURBO EXPO 2001, June, 4-7, 2001, New Orleans, 2001-GT-0406.

[9] D'Ovidio, A., Harkins, J.A., Gostelow, J.P., 2001 b "Turbulent spots in strong adverse pressure gradients part 2- Spot propagation and spreading rates," Proceedings of ASME Turbo Expo 2001, June 4-7 2001, New Orleans, 2001-GT-0406

[10] Stieger, R.D., 2002, "The effects of wakes on separating boundary layers in low pressure turbines," Ph.D.Thesis, Cambridge University, Cambridge

[11] LaVision, 2001, "DaVis Flowmaster," v. 6.03, February 2001, LaVision GmbH, Anna-VandenHoeck-Ring 19, 37081 Goettingen, FRG

[12] Meyer, R.X., 1958, "The Effects of Wakes on the Transient Pressure and Velocity Distributions in Turbomachines," ASME Journal of Basic Engineering, October, pp 1544-1552

[13] Stieger, R.D. and Hodson, H.P., 2003, "Unsteady Dissipation Measurements on a Flat Plate Subject to Wake Passing," submitted to 5th European Turbomachinery Conference, Prague

[14] Walker, G.J., 1989, "Transitional flow in axial turbomachine blading," AIAA Journal, **27** (5), pp 595-602

[15] Villermaux, E., 1998, "On the role of viscosity in shear instabilities," Phys. Fluids, **10**(2)

[16] Saathoff, P.J., and Melbourne, W.H., 1997, "Effects of free-stream turbulence on surface pressure fluctuations in a separation bubble," J. Fluid. Mech., **337**, pp1-24

[17] Luton, A., Ragab, S., Telionis, D,. 1995, "Interaction of spanwise vortices with a boundary layer," Phys. Fluids, **7**(11)

[18] Schubauer, G.B. and Skramstad, H.K., 1947, "Laminar boundary-layer oscillations and transition on a flat plate," NACA Report No. 909, 1947

[19] Watmuff, J. H., 1999, "Evolution of a wave packet into vortex loops in a laminar separation bubble," J. Fluid Mech., **397**, pp119-169

[20] Gaster, M., 1980, "On transition to turbulence in boundary layers", in "Transition and Turbulence," ed. R. E. Meyer, Proceedings of a Symposium, Conducted by the The Mathematics Research Centre, The University of Wisconsin-Maddison, October 13-15, 1980, Academic Press, 1981.